A KINETIC AND MORPHOLOGICAL STUDY OF DIAMOND INTERLAYER GROWTH

David S. Dandy,[1] Jungheum Yun,[1] and Pushpa Mahalingam[2]
[1] Dept. of Chemical Engineering, Colorado State University, Fort Collins, CO 80523
[2] Texas Instruments, 13121 TI Blvd., MS352, Dallas, TX 75243

A critical issue in diamond chemical vapor deposition is the inability of investigators to deposit heteroepitaxial films on carbide-forming substrates. One of the most common substrate materials, silicon, readily forms a thin, polycrystalline SiC layer when exposed to diamond growth conditions. It is not until the surface becomes saturated with carbon that diamond begins the nucleation and growth processes. Many attempts have been made to grow heteroepitaxial diamond films on silicon, but successful results are few and difficult to reproduce. Often, cross-section STM shows widely dispersed nanocrystals of heteroepitaxial diamond on silicon surrounded by a polycrystalline SiC film, on top of which grows a continuous, polycrystalline diamond film. In this work it is shown that it may be possible to exploit the ubiquitous SiC layer to grow, not single crystal diamond, but rather textured, highly oriented polycrystalline diamond. This would be carried out by careful control of the SiC interlayer growth step so that a desired SiC morphology is obtained.

INTRODUCTION

While diamond films are now routinely being synthesized by chemical vapor deposition (CVD) a number of experimental observations of diamond nucleation reveal that, in most cases, diamond does not nucleate directly on a non-diamond substrate surface. Instead, the diamond nucleates on an intermediate layer that develops at the interface between diamond and the non-diamond substrate. When diamond is grown on a carbide-forming substrate, silicon in this case, it is frequently observed that the interlayer is predominantly SiC (1–6). It is generally agreed that the SiC intermediate layer provides nucleation sites for diamond crystallite growth, enhances diamond nucleation densities on the silicon substrate, and provides an opportunity for controlling the morphology, orientation, and texture of diamond films during nucleation and growth (7). The formation of the interlayer is a necessary step in the spontaneous nucleation processes of diamond on non-diamond substrates, but it alone is not sufficient for diamond nucleation to occur (8). The formation rate and composition of the interlayer depends not only on the state of the silicon substrate but also on the deposition conditions. Silicon carbide is a thermodynamically preferred interlayer material, as will be discussed further, but depending on the inlet hydrocarbon concentration, reactor pressure, and substrate temperature, a non-diamond carbon phase may preferentially nucleate on the silicon substrate, followed by diamond nucleation and growth (9,10). Low inlet C:H ratio and/or high substrate temperature may favor the formation of SiC, while high inlet C:H ratio and/or low substrate temperature may lead to the formation of amorphous carbon or diamond like carbon (DLC), or even, possibly, the direct nucleation and growth of diamond on the silicon surface (11).

The issue then is, given the assumption that SiC readily forms on silicon substrates prior to diamond nucleation and growth, can this interlayer phase be exploited to control the morphology and texture of the diamond film? In principle, yes, if the morphology and texture of the SiC layer itself can be controlled. And, rather than passively obtaining the interlayer that forms on the substrate under conditions typical of the diamond nucleation stage, it may be possible to guarantee the formation of a crystalline SiC interlayer and to control its morphology through the active use of SiC precursors. Of the silicon carbide polytypes, β-SiC may be an ideal candidate for the interlayer phase because it readily grows on Si(100) substrates (12–21) and because of its cubic structure it has the potential to yield grain types and morphologies well suited for diamond growth.

As with any CVD process, the surface morphology of a continuous polycrystalline β-SiC interlayer is determined by the reactor operating conditions, particularly the substrate temperature and the inlet gas composition. At the present time, the effects of these operating parameters on the resulting surface morphology are not fully understood. An understanding of the relationships between operating conditions and film morphology may lead to optimal yield of interlayers that are highly $\langle 100 \rangle$-textured, with $\{100\}$ facets. Upon these layers diamond could nucleate and grow with good crystallographic registry.

The van der Drift model (22,23) represents a growth mechanism of continuous polycrystalline films from randomly oriented nucleated seed crystals. This model calculates the crystallographic texture and the surface morphology of the continuous polycrystalline film resulting from growth competition between nucleated seed crystals. As the film thickness increases and a continuous film is formed, those crystals having their fastest growth direction perpendicular to the substrate surface will overgrow all other orientations and the orientation of the crystals are represented on the surface. The model is expressed by the growth-rate parameter, $\alpha_{3D} = \sqrt{3}\,V_{100}/V_{111}$, where V_{100} and V_{111} are the growth velocities of the $\{100\}$ and $\{111\}$-facets. The α_{3D} value can be determined from the texture of a continuous polycrystalline film, assuming the absence of secondary nucleation and twinned crystals (23). After the film growth rate, V_{100}, is determined, the growth rate of $\{111\}$ face, V_{111}, can be calculated from the known values of α_{3D} and V_{100}.

Over the past several years X-ray diffraction (XRD) has been used to determine the effects of operating parameters on polycrystalline β-SiC film orientation. A number of investigators (12–21) have reported XRD data for the growth of β-SiC films on Si(100) substrates using a $SiH_4/C_3H_8/H_2$ inlet gas mixture. Using XRD, these investigators have examined the dependence of β-SiC morphology on substrate temperature and inlet Si:C atom ratio. Among these, Wu et al. (12) reported a series of XRD patterns of polycrystalline β-SiC films grown at substrate temperatures from 1263 K to 1433 K and a fixed inlet Si:C ratio of 0.42. They found that, while the preferred orientation of continuous polycrystalline films was (111) at 1323 K with negligible degree of (100) orientation, its orientation changed to (100) by increasing the substrate temperature to 1433 K.

Since two preferred surface orientations, $\{100\}$ and $\{111\}$, are usually observed in β-SiC growth on Si(100) substrates using a $SiH_4/C_3H_8/H_2$ inlet reactant gas mixture (12–21), the van der Drift model can be simplified to the growth of two-dimensional crystals. In a two-dimensional model, the growth parameter is defined as $\alpha_{2D} = \sqrt{2}\,V_{10}/V_{11}$, where V_{10} and V_{11} are the growth velocities of the $\{10\}$ and $\{11\}$ facets. This approach is re-

stricted to the situation where SiC is deposited on Si(100) substrates; when SiC is grown on Si(111), {110} and {111} orientations are typically observed.

Although it has been possible in the present study to correlate the growth parameter α_{2D} with operating conditions using published experiments, it has proven difficult to extract consistent growth rate data from the same body of work. In an attempt to quantify the dependence of growth rate on deposition conditions, Allendorf and Kee (24) calculated SiC growth rate as a function of substrate temperature and Si:C inlet atom ratio through the use of detailed gas-phase and surface chemical kinetic mechanisms. Allendorf and Kee considered steady state, rotating disk CVD of SiC from a SiH_4 and C_3H_8 mixture in H_2 carrier gas. Using the validated theoretical predictions of Allendorf and Kee, it has been possible to obtain realistic values for the growth rate of (100)β-SiC, and these are used, along with the experimentally determined values of α_{2D}, in a morphology evolution model to study the effect of operating conditions on film texture and roughness.

The purpose of the present work is to demonstrate that SiC will form preferentially relative to diamond on silicon substrates, and to predict the dependence of the surface morphology of β-SiC interlayers on the substrate temperature and inlet Si:C atom ratio. The evolution of SiC interlayer morphology will be simulated for different values of α_{2D} using a two-dimensional interface model. In this study, β-SiC interlayers grown on Si(100) substrates with a $SiH_4/C_3H_8/H_2$ inlet gas mixture are considered. The growth rates of the films are calculated from a rigorous transport and kinetic model applied to a pedestal reactor, using gas-phase momentum, mass, and energy conservation equations containing detailed homogeneous and heterogeneous chemistry.

MODEL DESCRIPTION

To predict the interlayer phase that will preferentially form on a silicon substrate, a quasi-equilibrium model has been applied to the SiC/graphite/diamond/H_2 system (25). The key assumption in the model is that thermochemical equilibrium conditions exist between the interlayer surface and the gas species adsorbing or desorbing from it. An advantage of the quasi-equilibrium approach over a purely kinetic method is the minimization of the use of kinetics to the degree that the rate expressions for the overall reactions are obtained without requiring knowledge of the detailed kinetic mechanisms of the deposition processes. Kinetic theory is used solely to obtain an expression for the rate at which gas molecules impinge upon the solid surface or desorb from the substrate. This expression corresponds to a boundary condition between the gas and solid phases, and it allows determination of the rates in terms of thermodynamic properties. The non-thermodynamic effect is accounted for by introducing adsorption and desorption probabilities into the model. The non-thermodynamic effect is due to only a certain fraction of the incident molecules being adsorbed on, and subsequently equilibrated with the interlayer surface, and the remainder simply scattered from the surface without undergoing chemical change. The predicted relative rates of carbon deposition and etching from SiC, graphite, and diamond indicate which interlayer phase is most likely to form. When the deposition/etching rates are evaluated at different inlet hydrocarbon concentrations and substrate temperatures a phase diagram can be constructed.

A different approach must be used to simulate the actual growth of the SiC interlayer and to examine the dependence of the growth rate on parameters such as substrate temperature and inlet Si:C atom ratio. To this end, a computer program (26) is used to compute gas-phase composition, temperature and velocity profiles, and deposition rates. The Fortran chemical kinetic codes called Chemkin-III (27) and Surface Chemkin (28) are used for the analysis of gas-phase and surface chemical kinetics. The gas-phase reaction and surface reaction mechanisms used in the calculations are simplified from those reported by Allendorf and Kee (24). The gas-phase multicomponent transport properties are calculated by using a computer package (29).

The evolution of surface morphology of two-dimensional polycrystalline β-SiC films is simulated by a two-dimensional numerical model, which is based on prescribed values of the growth rate parameter α_{2D} and the film growth rate, V_{10}, obtained from the pedestal reactor calculations. As an initial condition, randomly oriented seed crystals are placed at random locations on the substrate with average seed crystal separation d_0, and each face of each crystal is propagated over a finite time step using the prescribed α_{2D} and V_{10}.

RESULTS AND DISCUSSION

Interlayer Composition

The quasi-equilibrium model has been applied to predict the deposition conditions under which SiC and/or solid carbon phases such as graphite or diamond may form as interlayers on a silicon substrate. The range of substrate temperatures considered in the calculations is 500–1500 K for reactor pressures of 36 and 760 Torr. The pressures of 36 and 760 Torr have been chosen because these are representative of conditions under which both diamond and silicon carbide have been deposited. In Fig. 1, the predictions of the quasi-equilibrium model for the etching rates *E* of relevant species from the surfaces of SiC and solid carbon are shown as functions of the substrate temperature. Hydrocarbon species such as C_2H_2 that have been included in the model calculations but do not appear in Fig. 1 have etching rates negligible relative to those shown, or are etched at temperatures above 1500 K. The values of *E* shown in Fig. 1 correspond to a feed gas composition of 1% CH_4 in H_2 at a total pressure of 36 Torr.

In Fig. 1 the deposition rate of diamond and etching rates of molecular species from the diamond surface are plotted to allow comparison of the deposition of SiC and etching of species from SiC with those of diamond. As illustrated in Fig. 1, for graphite (C_g) and diamond (C_d) the dominant reaction product is CH_4 up to approximately 600 K, and H_2 dominates from 600 K to 1500 K. For SiC the dominant reaction product is always H_2 throughout the substrate temperature range for which results are reported. It may be seen in the figure that the etching rates of all hydrocarbon species from the SiC surface are below 10^{18} $cm^{-2}\,s^{-1}$. The calculations indicate that the partial pressures of the hydrocarbons etched from the possible interlayer phases increase in the order SiC < graphite < diamond. The reason for this trend in the partial pressures of etched species is due to the free energies of formation of SiC and the solid carbon phases, which vary as diamond > graphite > SiC. Since CH_4 is present in the incoming species flux, SiC or solid carbon will be deposited on the surface when the incoming carbon flux exceeds the flux of car-

bon leaving the surface due to etching. Under the condition of 1% CH_4 in H_2 at 36 Torr, graphite may be deposited for substrate temperatures greater than 900 K and diamond for temperatures greater than 1000 K, which SiC can, from a thermodynamic perspective, be deposited throughout the temperature range under consideration.

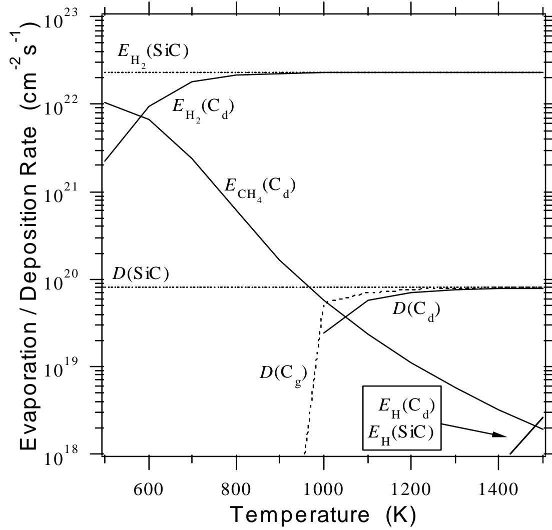

Figure 1. Model predictions for the etching rates (*E*) and deposition rates (*D*) of hydrocarbon species, SiC, diamond (C_d), and graphite (C_g).

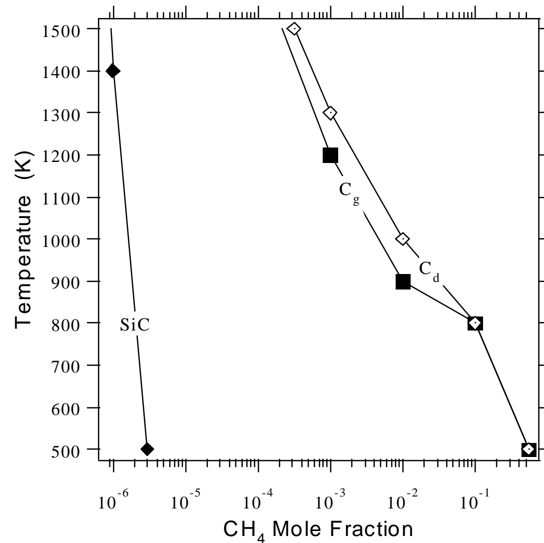

Figure 2. The predicted phase diagram for diamond (C_d), graphite (C_g), and SiC at a total system pressure of 36 Torr.

Evaluating carbon deposition and etch rates at 36 Torr for different inlet CH_4 concentrations and substrate temperatures leads to the phase diagram shown in Fig. 2. The boundary in the SiC/carbon-H phase diagram between etching and deposition of SiC or solid carbon corresponds to the locus of points for which the net deposition rate of that phase is identically zero; etching will occur to the left of the boundary while deposition occurs to the right. At a pressure of 36 Torr, the inlet CH_4 mole fraction required to deposit SiC, graphite, or diamond decreases with an increase in substrate temperature in the range $500 \leq T \leq 1500$ K. As illustrated in Fig. 2, the stability region of diamond lies within the stability region of SiC and graphite. In other words, the model predicts that whenever diamond can deposit, SiC or graphite may preferentially deposit.

Silicon Carbide Growth Rate

Although the surface reaction mechanism of β-SiC growth proposed by Allendorf and Kee (24) is somewhat complex, the mechanism can be simplified if the goal is solely to determine the growth rate. Numerical calculations have been performed to obtain a simplified surface reaction mechanism for β-SiC growth. The reaction rate of each elementary surface reaction has been evaluated to identify the predominant surface reactions from the detailed surface reaction mechanism. It is found that, among carbon-containing species, heterogeneous reactions involving CH_3, C_2H_2, and C_2H_4 are the most important, and among the Si-containing gas species, the heterogeneous reactions involving SiH_2 and Si are the most significant.

The growth rate of the SiC interlayer has been calculated at different substrate temperatures that are to be used in the two-dimensional morphology evolution model. In the growth model the substrate temperature is varied between 1323 K and 1623 K. The

growth model the substrate temperature is varied between 1323 K and 1623 K. The upper limit of 1623 K is chosen to avoid the melting point of the silicon substrate, which is 1683 K (24). Other operating conditions are chosen to match the experimental data of Wu et al. (12). The Si:C inlet atomic ratio is fixed at 0.42, a standard value in SiC deposition. The inlet mole fractions of SiH_4 and C_3H_8 are set to 2.0×10^{-4} and 1.6×10^{-4}. The inlet mole fraction ratio $H_2:(SiH_4 + C_3H_8) = 2780$. The predicted growth rate of β-SiC as a function of substrate temperature and inlet Si:C ratio is shown in Fig. 3. At lower temperatures, the strong dependence of β-SiC growth rate on temperature indicates that the growth rate is surface reaction rate limited, yielding an overall activation energy of approximately 4.5 kcal/mol. The dominant rate-limiting mechanism changes from the surface reaction rate to the mass transfer rate as the substrate temperature increases. This growth rate dependence on the substrate temperature is in reasonable agreement with the results of Wu et al. (12). As can be seen in Fig. 3(b), the system is mass transfer limited in the silicon precursor species when the inlet Si:C ratio falls below 0.6.

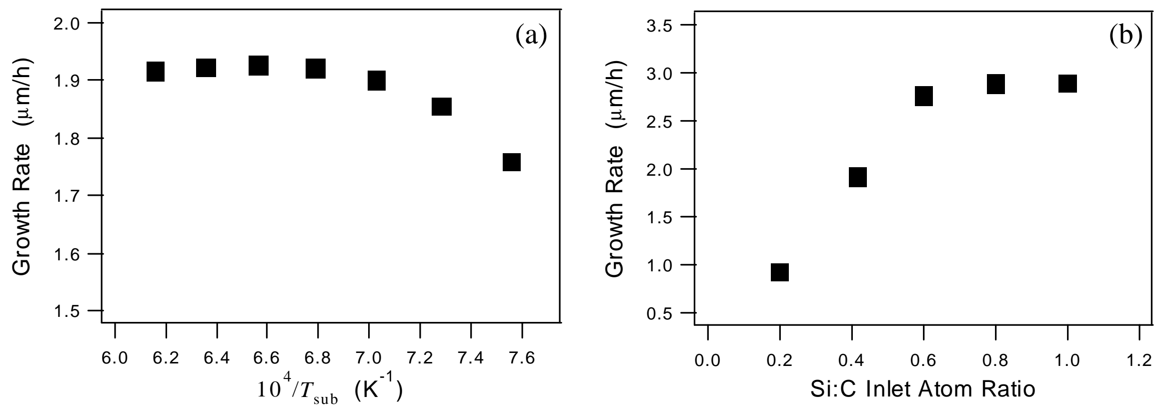

Figure 3. The growth rate of a β-SiC interlayer as a function of (a) the substrate temperature and (b) the inlet Si:C atom ratio, for the following operating conditions: $T_{inlet} = 300$ K; $P = 760$ Torr; $U_{inlet} = 2.5$ cm/s; and inlet mole fractions $X_{H_2} = 0.9964$, $X_{SiH_4} = 2\times10^{-4}$, $X_{C_3H_8} = 1.6\times10^{-4}$.

Film Morphology Evolution

From experimental observation (12) it may be concluded that the increase of the growth rate parameter α_{2D} from 1 to 1.95 is primarily due to an increase in the substrate temperature from 1323 K to 1423 K. The effect of Si:C inlet atom ratio on α_{2D} does not appear to be important because the experiments (12–21) indicate that, for inlet Si:C atom ratios ranging from 0.3 to 0.83, β-SiC films have (100) film texture for substrate temperatures above 1423 K.

A two-dimensional front-vertex tracking model has been used to calculate the surface morphology of polycrystalline β-SiC interlayers based on the growth rate parameter α_{2D} and the predicted growth rate of (10)β-SiC. It is calculated that, when α_{2D} is unity at a substrate temperature of 1323 K, the surface facets on a thin film (thickness $10\,d_0$, where d_0 is the average distance between seed crystals) are randomly oriented because each of the nucleated seed crystals is placed on the substrate surface with random orientation. However, the film texture has mainly ⟨11⟩ direction and this texture leads to mainly {11} facets on the surface of thicker films (thickness > $200\,d_0$). When $\alpha_{2D} = 1.95$ at the substrate temperature of 1423 K, a small fraction of {10}-facets is observed in thin layers

($10\,d_0$). The formation of {10}-facets continues as the film grows, eventually reaching a morphology where the surface facets are primarily {10}. Figure 4 shows the dependence of the surface roughness, measured as the average peak-to-valley height, on the film thickness and α_{2D} value. The surface roughness significantly increases with increasing the film thickness for both α_{2D} values. However, when $\alpha_{2D} = 1.95$, the surface morphology of the film is smoother than that for $\alpha_{2D} = 1.0$. This result suggests that the {10}-facets result in an increasingly smoother surface morphology. The evolution of the relative size of the $\langle 10 \rangle$- and $\langle 11 \rangle$-oriented grain and average grain size are shown in Fig. 5. When $\alpha_{2D} = 1.95$, the average grain size increases with increasing the film thickness as expected, and the grain size ratio $\langle 10 \rangle / \langle 11 \rangle$ also increases with film thickness because the preferred $\langle 10 \rangle$ orientation of the crystallite continues to evolve for this value of α_{2D}. As can be seen in Fig. 5, the evolution of grain size follows the expected square root scaling with film thickness.

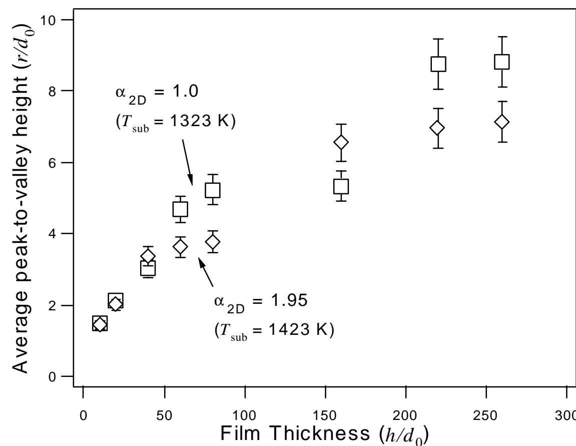

Figure 4. Predicted surface roughness as a function of film thickness for different α_{2D} values.

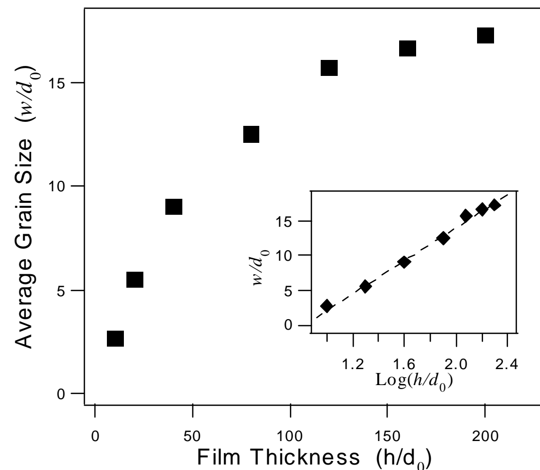

Figure 5. Evolution of the average grain size with the film thickness for $\alpha_{2D} = 1.95$.

SUMMARY

The interlayer that forms at the interface between diamond and a silicon substrate during diamond CVD has been analyzed using a thermodynamic quasi-equilibrium model. The model predicts the preferential formation of SiC on silicon substrates for typical diamond CVD nucleation and growth conditions. The model also predicts that, for growth of diamond, graphite, and SiC, the required inlet CH_4/H_2 ratio varies directly with reactor pressure and inversely with substrate temperature. The calculations are in qualitative agreement with experimental and theoretical results available in the literature.

Calculations have also been performed to determine the growth rate of a (100)β-SiC interlayer and the evolution of film morphology of a continuous polycrystalline SiC interlayer. The dependences of growth rate and morphology on substrate temperature and inlet reactant composition have been examined. A two-dimensional morphology evolution model has been used to calculate the texture, surface roughness, and grain size of continuous polycrystalline β-SiC films. The results indicate that the surface morphology and the film texture of β-SiC are strongly affected by the substrate temperature. The results also determine the operating conditions optimizing the smoothness of surface morphology of β-SiC.

REFERENCES

1. S.D. Wolter, J.T. Glass, and B.R. Stoner, *J. Appl. Phys.,* **77**, 5119 (1995).
2. S.D. Wolter, B.R. Stoner, J.T. Glass, P.J. Ellis, D.S. Buhanenko, C.E. Jenkins, and P. Southworth, *Appl. Phys. Lett.,* **62**, 1215 (1993).
3. D. Kim, H. Lee, and J. Lee, *J. Mater. Sci.,* **28**, 6704 (1993).
4. B.R. Stoner, S.R. Sahaida, J.P. Bade, P. Southworth, and P.J. Ellis, *J. Mater. Res.,* **8**, 1334 (1993).
5. M.M. Waite and S.I. Shah, *Appl. Phys. Lett.,* **60**, 2344 (1992).
6. G.A. Hirata, L. Cota-Araiza, M. Avalos-Borja, M.H. Farias, O. Contreras, and Y. Matsumoto, *J. Phys.,* **5**, A305 (1993).
7. D. Michau, B. Tanguy, G. Demazeau, M. Couzi, and R. Cavagnat, *Diam. Related Mater.,* **2**, 19 (1993).
8. B.R. Stoner, G.H.M. Ma, S.D. Wolter, and J.T. Glass, *Phys. Rev. B,* **45**, 11067 (1992).
9. P.N. Barnes and R.L.C. Wu, *Appl. Phys. Lett.,* **62**, 37 (1993).
10. K. Tamaki, Y. Watanabe, Y. Nakamura, and S. Hirayama, *Thin Solid Films,* **236**, 115 (1993).
11. H. Liu and D.S. Dandy, *Diamond Chemical Vapor Deposition: Nucleation and Early Growth Stages,* Noyes Publications, Pennington, NJ (1995).
12. C. H. Wu, A. J. Fleischman, C. A. Zorman, and M. Mehregany, *Mater. Sci. Forum*, **264–268**, 179 (1998).
13. M. I. Chaudhry and R. L. Wright, *J. Mater. Res.*, **5**, 1595 (1990).
14. A. J. Steckl and J. P. Li, *IEEE Trans. Electron. Devices*, **39**, 64 (1992).
15. C. A. Zorman, A. J. Fleischman, A. S. Dewa, M. Mehregany, C. Jacob, S. Nishino, and P. Pirouz, *J. Appl. Phys.*, **78**, 5136 (1995).
16. S. Nishino, J. A. Powell, and H. A. Will, *Appl. Phys. Lett.*, **42**, 460 (1983).
17. P. E. R. Nordquist, G. Kelner, M. L. Gipe, and P. H. Klein, *Mater. Lett.*, **8**, 209 (1989).
18. O. Kordina, L. O. Björketun, A. Herry, C. Hallin, R. C. Glass, L. Hultman, J. E. Sundgren, and E. Janzen, *J. Cryst. Growth*, **154**, 303 (1995).
19. K. Shibahara, S. Nishino, and H. Matsunami, *J. Cryst. Growth*, **78**, 538 (1986).
20. M. I. Chaudhry, R. J. McCluskey, and R. L. Wright, *J. Cryst. Growth*, **113**, 120 (1991).
21. J. D. Hwang, Y. K. Fang, Y. J. Song, and D. N. Yaung, *Thin Solid Films*, **272**, 4 (1996).
22. C. Wild, N. Herres, and P. Koidl, *J. Appl. Phys.*, **68**, 973 (1990).
23. C. Wild, P. Koidl, W. Müller-Sebert, H. Walcher, R. Kohl, N. Herres, R. Locher, R. Samlenski, and R. Brenn, *Diamond Relat. Mater.,* **2**, 158 (1993).
24. M. D. Allendorf and R. J. Kee, *J. Electrochem. Soc.*, **138**, 841 (1991).
25. P. Mahalingam and D.S. Dandy, *Thin Solid Films,* **322**, 108 (1998).
26. M. E. Coltrin, R. J. Kee, G. H. Evans, E. Meeks, F. H. Rupley, and J. F. Grear, *Report No. SAND 91-8003* (1991).
27. R. J. Kee, F. M. Rupley, and J. A. Miller, *Report No. SAND 89-8009B* (1993).
28. M. E. Coltrin, R. J. Kee, and F. M. Rupley, *Report No. SAND 90-8003B* (1991).
29. R. J. Kee, G. Dixon-Lewis, J. Warnatz, M. E. Coltrin, and J. A. Miller, *Report No. SAND 86-8246* (1986).